

Cite this: *RSC Adv.*, 2017, 7, 20354

H-Shape mesogenic dimers – the spacer parity effect†

J. M. Wolska, M. Kolpaczynska, J. Mieczkowski, D. Pocięcha and E. Gorecka

It was found that for H-shape dimers, the parity of the number of atoms in the spacer linking the mesogenic cores has important influence on the mesogenic properties only for the molecules with weak mesogenic core anisotropy. In the case of stronger core anisotropy, the parallel arrangement of mesogenic units is induced regardless of the spacer parity. As a result, phase transition temperatures and layer spacing are only weakly affected by spacer parity. By studying the properties of six new homologue series it was found that for H-shape dimers the orthogonal smectic (SmA) is strongly disfavoured: most compounds form a tilted smectic (SmC) phase, which is related to hindrances in molecular rotation for molecules with large breadth to length ratio. For dimers with very long spacer, and thus decoupled mesogenic units, the smectic phase is replaced by a nematic phase, and for stiff polycatenar molecules with very short spacers the cubic phase can appear.

Received 6th March 2017
Accepted 31st March 2017

DOI: 10.1039/c7ra02730c

rsc.li/rsc-advances

Introduction

Liquid crystalline dimers and oligomers, as compounds with intermediate structures between monomers and polymers, have always been an important class of mesogenic compounds. Their unique properties result from the additional degree of freedom due to the presence of flexible chain linking mesogenic cores.^{1–3} Dimers often exhibit phases rarely observed for monomers; they easily form modulated smectics,⁴ polar smectics⁵ and broken-layer type columnar phases;⁶ there is also a limited number of reports that dimers might exhibit cubic phases.⁷ As mesogenic cores the rod-like,^{2,3,8} disc-like⁹ or bent-shape¹⁰ units were applied in molecular design. For the most studied dimers, with end-to-end connected rod-like mesogenic units, it was found the number of atoms in spacer is of primary importance for the type of the phase formed as well as transition temperatures.^{2,3,11} The parity of spacer affects the overall molecular shape² (Fig. 1), for even number of atoms in the spacer molecules adopt zigzag geometry, in which the mesogenic units are anti-parallel, whereas the spacer with odd number of atoms results in bent shape of the molecule, with the mesogenic units being inclined to each other.^{2,3} The interest in dimers having bent shape was strongly stimulated by recent discovery of twist-bend nematic (N_{TB}) phase, the heliconical phase made by achiral molecules.^{8,12} Apart of dimers, in which two mesogenic

cores are connected end-to-end also other molecular geometries were recently investigated, *e.g.* T-shape,¹³ U-shape¹⁴ or H-shape¹⁵ molecules (Fig. 1).

Herein, we describe 6 new series of laterally linked, symmetric dimeric molecules (H-shape), built of rod-like mesogenic cores interconnected through flexible alkoxy spacers of different length ($n = 1, 3–10$) (Scheme 1).

The rod-like units having different number of phenyl rings were used in order to study influence of geometrical anisotropy of mesogenic core on the phase properties. Further modification of molecular geometry was obtained by a variation of number and length of terminal chains. The phase transition temperatures for studied materials were collected in Tables 1–6 and the phase sequences are presented in Fig. 2.

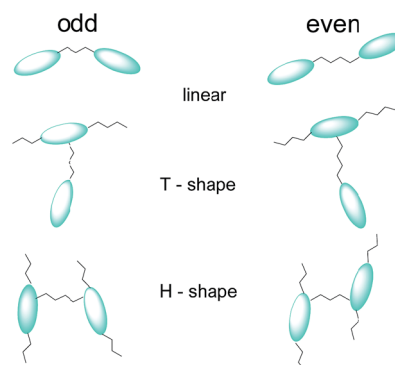
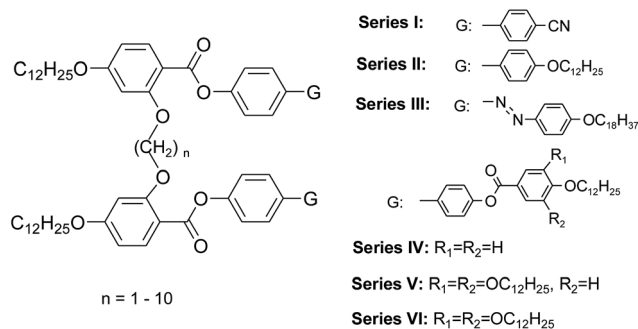


Fig. 1 Types of dimers and different conformations of molecules due to the odd–even effect.

Department of Chemistry, Warsaw University, Pasteura 1, 02-093 Warsaw, Poland.
E-mail: jokos@chem.uw.edu.pl; Tel: +48 22 5526270

† Electronic supplementary information (ESI) available: Chemical characterization of obtained materials and detailed description of experimental methods used for structure studies. See DOI:10.1039/c7ra02730c



Scheme 1 Molecular structures of the investigated compounds.

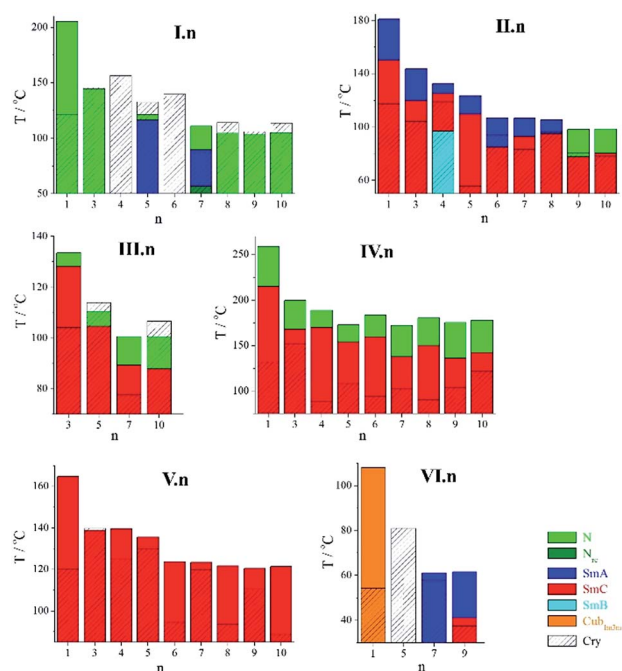


Fig. 2 Phase diagrams for the studied homologue Series I–VI.

Results and discussion

Most of the compounds of **Series I** with simple cyanobiphenyl unit in the mesogenic cores exhibited liquid crystalline phases (Table 1, Fig. 2) except those with short even spacers ($n = 4, 6$).

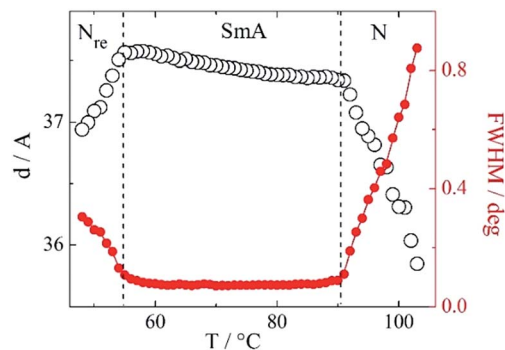


Fig. 3 Smectic layer spacing and width of corresponding diffraction signal vs. temperature for compound I.7.

For longer homologues with even spacers, monotropic nematic phase was observed. Molecules with odd spacers, in general, had better mesogenic properties, they all formed nematic phase, and additionally for homologues $n = 5$ and 7 a partially bilayer smectic A_d phase was found, with the layer spacing d slightly larger than the estimated molecular length ($d/L \sim 1.1$). Interestingly, compound **I.7** exhibited rare, for dimers, phase sequence with re-entrant nematic phase (N_{re}) formed below the smectic A_d phase. The N - SmA_d - N_{re} phase sequence has been confirmed by XRD measurements, the transitions between smectic and nematic phases were signified by the broadening of the diffraction signal related to the lamellar structure, due to the loss of long-range positional order (Fig. 3). The half-width of XRD signal measured in both nematic phases was similar (Fig. 3), indicating comparable correlation length of positional order in N and N_{re} phases.

The phase properties of homologues of the **Series II**, having the dodecyloxy chains instead of CN group, attached to the biphenyl units are collected in Table 2.

Compounds **II.1–II.8** exhibited the SmA - SmC phase sequence on cooling, while for the longest spacer homologues, **II.9–II.10**, a SmA phase was replaced by nematic phase. The richest polymorphism was found for even spacer compound **II.4**, which formed additional orthogonal smectic B phase below the SmC , however monotropic character of the phase prevented its detailed characterization. The temperature dependence of smectic layer thickness evaluated from XRD experiments confirmed continuous character of the SmA - SmC phase transition (Fig. 4) for all the homologues. Clear odd-even effect

Table 1 Series I phase transitions temperatures (in °C) and in parenthesis transition enthalpies (in kJ mol⁻¹)

I.n	mp	N_{re}	SmA	N	Iso
I.1	121.7 (66.4)			●	205.2 (2.1)
I.3	145.6 (79.8)			●	144.4 (2.0)
I.4	156.4 (108.4)				
I.5	132.8 (83.4)		●	●	121.8 (1.9)
I.6	139.8 (41.0)				
I.7	87.9 (78.5)	●	56.7 (0.1)	●	110.8 (0.1)
I.8	114.4 (58.1)			●	104.5 (0.7)
I.9	106.2 (80.6)			●	103.6 (0.9)
I.10	113.8 (81.3)			●	105.0 (0.7)



Table 2 Series II – phase transitions temperatures (in °C) and in parenthesis transition enthalpies (in kJ mol⁻¹)

II.n	mp	SmB	SmC	SmA	N	Iso
II.1	117.6 (37.5)		●	150 ^a	●	181.0 (14.8)
II.3	104.3 (77.2)		●	120 m	●	143.7 (16.8)
II.4	118.9 (111.7)	●	96.7 (14.1)	●	125 m	●
II.5	122.0 (49.6)		●	114.5 (0.1)	●	124.6 (15.2)
II.6	94.2 (74.3)		●	85 m	●	106.9 (4.0)
II.7	83.1 (79.6)		●	93 m	●	106.6 (9.4)
II.8	96.6 (86.7)		●	95 m	●	105.6 (8.6)
II.9	80.3 (35.8)		●	77.6 (0.1)	●	98.3 (3.6)
II.10	78.3 (56.0)		●	80.4 (0.4)	●	98.4 (3.4)

^a From microscopic observations.

regarding the layer spacing in smectic phase was observed (Fig. 4), even spacer homologues showed slightly larger *d* values.

For all the homologues the layer spacing was found to be much smaller than molecular length (estimated to be ~60 Å for even spacer and ~50 Å for odd spacer homologues) showing strong interdigitation of terminal chains between neighbouring layers. In SmA phase the layer expansion is negative and similar for all materials, while the thermal expansion coefficient in SmC phase changes its sign upon elongation of the spacer, on heating, far from SmA phase transition temperature, the contraction of the layers was found for compounds II.1 and II.3, and for longer homologues layer thickness monotonically increased in whole temperature range (Fig. 4). The effect might be explained by different degree of terminal chain interdigitation between layers, that is more significant for molecules with longer spacer between mesogenic cores.

For compounds of Series III, the azo group was introduced into mesogenic core, such elongation of mesogenic core resulted in destabilization of the SmA phase on behave of nematic phases, the phase sequence with N and SmC phase was observed for all homologues (Table 3). Due to the presence of azo group the materials were photosensitive, absorption of UV light caused the *trans-cis* isomerization of azo unit (see ESI†) that disrupted the mesogenic properties.

Elongation of the rigid mesogenic cores by additional phenyl ring attached to biphenyl unit through the ester linkage (Series IV) caused strong increase of liquid crystalline phases stability, the clearing temperatures for compounds IV.n were higher by more than 50 K comparing to their II.n analogues.

All the compounds of Series IV exhibited similar LC polymorphism, smectic C and nematic phases were observed (Table 4). Contrary to Series II, for the homologues of Series IV clear odd-even effect was found regarding the phase transition temperatures, the effect is clearly visible for intermediate homologues (Fig. 2), interestingly changing the parity of the linkage chain has opposite influence on the melting and clearing temperatures – the clearing temperature of even spacer homologues was higher while melting temperature lower than for odd spacer compounds.

Further modification of the molecular architecture by attaching additional terminal dodecyloxy chains (one in Series V and two in Series VI) to each mesogenic core resulted in destabilization of LC phases; lowering of the clearing

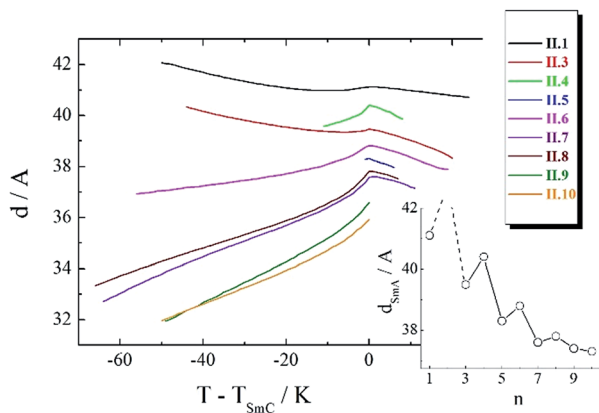


Fig. 4 Smectic layer spacing vs. temperature for homologues II.n. In the inset the layer spacing in SmA phase at the transition to SmC phase vs. spacer length, *n*.

Table 3 Series III – phase transitions temperatures (in °C) and in parenthesis transition enthalpies (in kJ mol⁻¹)

III.n	mp	SmC	N	Iso
III.3	104.3 (89.3)	●	128.3 (0.3)	●
III.5	114 (161.4)	●	104.7 (1.0)	●
III.7	77.6 (105.5)	●	89.5 (0.3)	●
III.10	106.7 (139.0)	●	87.9 (1.8)	●

Table 4 Series IV phase transitions temperatures (in °C) and in parenthesis transition enthalpies (in kJ mol⁻¹)

IV.n	mp	SmC	N	Iso
IV.1	132.5 (59.3)	●	215.2 (4.2)	●
IV.3	152.2 (75.2)	●	167.8 (2.9)	●
IV.4	88.3 (17.9)	●	170.1 (6.1)	●
IV.5	108.4 (24.9)	●	154.3 (5.0)	●
IV.6	94.3 (21.0)	●	159.8 (5.2)	●
IV.7	102.7 (25.1)	●	137.8 (5.1)	●
IV.8	90.4 (54.6)	●	150.3 (3.5)	●
IV.9	103.6 (38.3)	●	136.0 (3.7)	●
IV.10	122.1 (84.8)	●	142.5 (3.3)	●



Table 5 Series V phase transitions temperatures (in °C) and in parenthesis transition enthalpies (in kJ mol⁻¹)

V.n	mp	SmC		Iso
V.1	120.2 (69.2)	●	164.9 (8.3)	●
V.3	140.0 (69.2)	●	138.8 (24.6)	●
V.4	125.0 (14.7)	●	139.6 (22.3)	●
V.5	130.1 (6.6)	●	135.6 (15.3)	●
V.6	95.0 (52.4)	●	123.7 (20.0)	●
V.7	119.8 (52.0)	●	123.3 (21.6)	●
V.8	93.7 (41.1)	●	121.7 (14.7)	●
V.9	110.3 (37.5)	●	120.5 (20.5)	●
V.10	88.9 (34.9)	●	121.4 (21.0)	●

Table 6 Series VI phase transitions temperatures (in °C) and in parenthesis heat transition enthalpies (in kJ mol⁻¹)

VI.n	mp	SmC	SmA	Cub _{Im3m}	Iso
VI.1	54.1 (80.8)			●	108.0 (3.9) ●
VI.5	80.9 (13.2)				●
VI.7	57.6 (52.9)		●	61.0 (2.1)	●
VI.9	37.4 (94.8)	●	41.1 (1.6)	61.4 (3.1)	●

temperature was the strongest in case of molecules with three dodecyloxy chains. Compounds of **Series V** showed exclusively tilted smectic C phase, with clearing temperatures lower by 40–90 K in comparison to analogue compounds of **Series IV**; while an orthogonal smectic A phase was observed for two homologues of **Series VI** with long spacers $n = 7$ and 9.

For the compound **VI.1**, with three terminal chains and the shortest linkage, another type of LC phase was found – instead of lamellar phases, a cubic LC phase was formed. The phase was

optically isotropic, while the XRD experiments indicated presence of long-range positional order of molecules. The XRD patterns showed series of sharp diffraction signals at low angle range and a diffused signal at the high angle range proving the liquid crystalline character of the phase (Fig. 5). The best fitting of the low-angle part of the diffractogram was obtained assuming 3D crystallographic lattice of $Im3m$ symmetry and lattice parameter $a = 176.8$ Å (at $T = 50$ °C), corresponding roughly to 3 molecular lengths. Assuming the density of the cubic phase 1 g cm^{-3} , the number of dimeric molecules in the unit cell was estimated to be as high as 1440.

Experimental

Synthetic procedures

Detailed synthetic procedures are shown in Scheme 2. **Series I–VI** were prepared by condensation of two parts: rod-like ligands providing liquid crystalline properties of final compounds, and H-shaped dimeric units with an alkyl spacer providing odd–even behavior. **Series I** was prepared with commercially available 4-cyanobiphenol (**9**). The 4,4'-biphenol (**1**) was used as a main rigid fragment of rod-like compounds. The one exemption was 4-hydroxy-4'-(4-octadecyloxy)diazobenzene (**12**) prepared in 3-steps: alkylation of 4-nitrophenol, reduction of nitro group to amine group (**11**), and final azo coupling with phenol (**12**). All alkoxy derivatives were obtained *via* Williamson reaction, carried out in anhydrous DMF in presence of KI and K₂CO₃ (a). All ester derivatives were prepared by esterification reaction in anhydrous THF in presence of TEA and DMAP (b). The compounds were purified by recrystallization from MeOH, toluene, hexane or by column chromatography using CH₂Cl₂, toluene, and mixture of MeOH/CHCl₃ as eluents. All H-shaped units were prepared *via* alkylation reaction of ethyl 4-dodecyloxy-2-hydroxybenzoate (**13**) with appropriate dihalogenic alkanes. Hydrolysis and further acylation reaction allowed receiving H-shaped acidic chlorides (**16/n**) common for all **Series I–VI** and used in final esterification reaction with characteristic rod-like ligands. For more details see ESI.†

Materials and methods

Temperatures and thermal effects of the phase transitions were determined by calorimetric studies using TA Q200 calorimeter, samples of mass 1–3 mg were sealed in aluminum pans and kept in nitrogen atmosphere during measurement. Both heating and cooling scans with rate 10 K min^{-1} were applied. The optical studies were performed using Zeiss Imager A2m polarizing microscope equipped with Linkam heating stage. The small angle X-ray diffraction patterns were obtained with Bruker Nanostar system (CuK α radiation, three pinhole collimation system, area detector VANTEC 2000, MRI TCP-U heating stage), while wide angle diffraction experiments were performed with Bruker GADDS diffractometer (CuK α radiation, point collimator, Vantec 2000 area detector, modified Linkam heating stage). Samples were prepared in a form of droplet on heated surface, their temperature was controlled with precision 0.1 K. For UV-vis experiment the Shimadzu UV-3101PC spectrometer

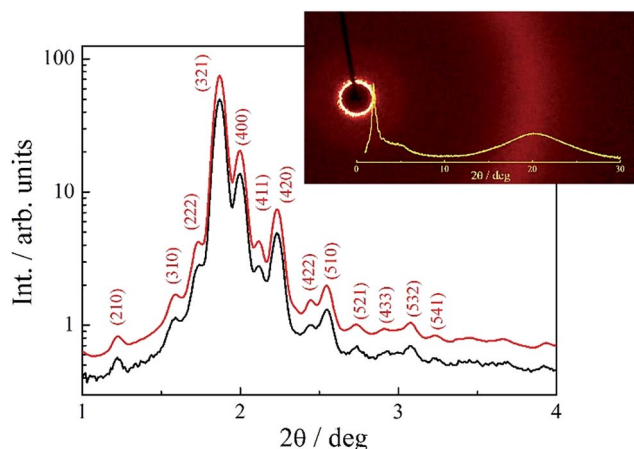


Fig. 5 Low angle X-ray diffractogram (black line) registered for compound **VI.1** at 50 °C. The fitting curve (red line) was obtained assuming crystallographic lattice with $Im3m$ symmetry and unit cell parameter $a = 176.8$ Å. In the inset 2D XRD pattern recorded in broad diffraction angle range; diffused high angle signal evidences liquid crystalline character of the phase.



Notes and references

- 1 C. T. Imrie and G. R. Luckhurst, *Handbook of Liquid Crystals*, Wiley-VCH, Weinheim, 2014, vol. 7, pp. 137–210, and references cited therein.
- 2 C. T. Imrie and P. A. Henderson, *Chem. Soc. Rev.*, 2007, **36**, 2096.
- 3 P. A. Henderson and C. T. Imrie, *Liq. Cryst.*, 2011, **38**, 1407.
- 4 D. Chen, M. Nakata, R. Shao, M. R. Tuchband, M. Shuai, U. Baumeister, W. Weissflog, D. M. Walba, M. A. Glaser, J. E. MacLennan and N. A. Clark, *Phys. Rev. E: Stat., Nonlinear, Soft Matter Phys.*, 2014, **89**, 022506; D. Pociecha, D. Kardas, E. Gorecka, J. Szydłowska, J. Mieczkowski and D. Guillon, *J. Mater. Chem.*, 2003, **13**, 34.
- 5 Y. Shimbo, E. Gorecka, D. Pociecha, F. Araoka, M. Goto, Y. Takanishi, K. Ishikawa, J. Mieczkowski, K. Gomola and H. Takezoe, *Phys. Rev. Lett.*, 2006, **97**, 113901; J. Mieczkowski, K. Gomola, J. Koseska, D. Pociecha, J. Szydłowska and E. Gorecka, *J. Mater. Chem.*, 2003, **13**, 2132; H. N. S. Murthy, M. Bodyagin, S. Diele, U. Baumeister, G. Pelzl and W. Weissflog, *J. Mater. Chem.*, 2006, **16**, 1634.
- 6 Y. Takanishi, M. Toshimitsu, M. Nakata, N. Takada, T. Izumi, K. Ishikawa, H. Takezoe, J. Watanabe, Y. Takahashi and A. Iida, *Phys. Rev. E: Stat., Nonlinear, Soft Matter Phys.*, 2006, **74**, 051703; T. Izumi, Y. Naitou, Y. Shimbo, Y. Takanishi, H. Takezoe and J. Watanabe, *J. Phys. Chem. B*, 2006, **110**, 23911.
- 7 B.-K. Cho, J.-H. Ryu, W.-C. Zin and M. Lee, *Polym. Bull.*, 2000, **44**, 393; T. Kajitani, S. Kohmoto, M. Yamamoto and K. Kishikawa, *Chem. Mater.*, 2005, **17**, 3812; J. M. Wolska, D. Pociecha, J. Mieczkowski and E. Gorecka, *Liq. Cryst.*, 2016, **43**, 235.
- 8 M. G. Tamba, S. M. Salili, C. Zhang, A. Jakli, G. H. Mehl, R. Stannarius and A. Eremin, *RSC Adv.*, 2015, **5**, 11207; M. Cestari, S. Diez-Berart, D. A. Dunmur, A. Ferrarini, M. R. de la Fuente, D. J. B. Jackson, D. O. Lopez, G. R. Luckhurst, M. A. Perez-Jubindo, R. M. Richardson, J. Salud, B. A. Timimi and H. Zimmermann, *Phys. Rev. E: Stat., Nonlinear, Soft Matter Phys.*, 2011, **84**, 031704; V. Borshch, Y.-K. Kim, J. Xiang, M. Gao, A. Jakli, V. P. Panov, J. K. Vij, C. T. Imrie, M. G. Tamba, G. H. Mehl and O. D. Lavrentovich, *Nat. Commun.*, 2013, **4**, 2635.
- 9 T. Sakurai, K. Tashiro, Y. Honsho, A. Saeki, S. Seki, A. Osuka, A. Muranaka, M. Uchiyama, J. Kim, S. Ha, K. Kato, M. Takata and T. Aida, *J. Am. Chem. Soc.*, 2011, **133**, 6537; J. Vergara, J. Barbera, J. L. Serrano, M. B. Ros, N. Sebastian, R. de la Fuente, D. O. Lopez, G. Fernandez, L. Sanchez and N. Martin, *Angew. Chem., Int. Ed.*, 2011, **50**, 12523.
- 10 N. Sebastián, N. Gimeno, J. Vergara, D. O. Lopez, J. L. Serrano, C. L. Folcia, M. R. de la Fuente and M. B. Ros, *J. Mater. Chem. C*, 2014, **2**, 4027; C. M. Heggulustoy, M. B. Darda, R. S. Montani, B. Heinrich, B. Donnio, D. Guillon and R. O. Garay, *Liq. Cryst.*, 2015, **42**, 1013; M. Horcic, J. Svoboda, V. Novotna, D. Pociecha and E. Gorecka, *Chem. Commun.*, 2017, **53**, 2721.
- 11 R. W. Date, C. T. Imrie, G. R. Luckhurst and J. M. Seddon, *Liq. Cryst.*, 1992, **12**, 203.
- 12 D. Chen, J. H. Porada, J. B. Hooper, A. Klitnick, Y. Shen, M. R. Tuchband, E. Korblova, D. Bedrov, D. M. Walba, M. A. Glaser, J. E. MacLennan and N. A. Clark, *Proc. Natl. Acad. Sci. U. S. A.*, 2013, **110**, 15931.
- 13 A. Yoshizawa, M. Sato and J. Rokunohe, *J. Mater. Chem.*, 2005, **15**, 3285.
- 14 G. S. Attard and A. G. Douglass, *Liq. Cryst.*, 1997, **22**, 349.
- 15 W. Weissflog, D. Demus, S. Diele, P. Nitschke and W. Wedler, *Liq. Cryst.*, 1989, **5**, 111; S.-M. Huh and J.-I. Jin, *Liq. Cryst.*, 1998, **25**, 285; W. Wedler, D. Demus, H. Zashcke, K. Mohr, W. Schafer and W. Weissflog, *J. Mater. Chem.*, 1991, **1**, 347; W.-S. Bae, J.-W. Lee and J.-I. Jin, *Liq. Cryst.*, 2001, **28**, 59; J. Andersch, C. Tschierske, S. Diele and D. Lose, *J. Mater. Chem.*, 1996, **6**, 1297; B. Kumar, A. K. Prajapati, M. C. Varia and K. A. Suresh, *Langmuir*, 2009, **25**, 839; Y. Zhang, J. Martinez-Perdiguerro, U. Baumeister, C. Walker, J. Etxebarria, M. Prehm, J. Ortega, C. Tschierske, M. J. O'Callaghan, A. Harant and M. Handschy, *J. Am. Chem. Soc.*, 2009, **131**, 18386; A. K. Prajapati, M. C. Varia and S. P. Sahoo, *Liq. Cryst.*, 2011, **38**, 861; M. Kolpaczynska, K. Madrak, J. Mieczkowski, E. Górecka and D. Pociecha, *Liq. Cryst.*, 2011, **38**, 149; T. Sakurai, K. Tashiro, Y. Honsho, A. Saeki, S. Seki, A. Osuka, A. Muranaka, M. Uchiyama, J. Kim, S. Ha, K. Kato, M. Takata and T. Aida, *J. Am. Chem. Soc.*, 2011, **133**, 6537; J. Vergara, J. Barbera, J. L. Serrano, M. B. Ros, N. Sebastian, R. de la Fuente, D. O. Lopez, G. Fernandez, L. Sanchez and N. Martin, *Angew. Chem., Int. Ed.*, 2011, **50**, 12523.

